Evaluation of the performance of circular hollow section joints reinforced by stiffened plates under fatigue loadings

L.M. El-Hifnawy, E.A. Mashaly, M.M. El-Heweity and T.M. Ragab

Structural Eng. Dept., Faculty of Eng., Alexandria University, Alexandria, Egypt

The aim of this paper is to evaluate the performance of Circular Hollow Section (CHS) joints reinforced by stiffened plates under fatigue loadings. This is done by studying the Stress Concentration Factors (SCFs) of stiffened tubular joints subjected to various types of basic loadings such as axial force, in plane and out-of-plane bending moments. The finite element method is adopted in the numerical parametric studies to calculate the SCFs. To verify the numerical results, the results of unstiffened joints are compared with those of the empirical formulae available in the literature. After the verification, a parametric study is generated in order to evaluate the performance of stiffeners in CHS joints. The parametric study is done by varying the geometrical parameters of the joints such as the wall thickness ratio and the diameter ratio between the brace and the chord members of the joints. Also, the variation of the thickness of the stiffened plate as a ratio from the chord thickness is considered in the parametric study. From the results obtained, the stress concentration factors in the stiffened joints were found lower than in the unstiffened joints which enhance the performance of joints under fatigue loadings.

يهدف هذا البحث الى تقييم اداء الوصلات ذات القطاعات الدائرية المفرغة المقواه بألوح تقوية تحت تأثير أحمال التعب. وقد تم هذا عن طريق دراسة معاملات تركيز الاجهادات للوصلات المقواه تحت تأثير أحمال أساسية مختلفة مثل القوة المحورية، عزوم فى المستوى وعزوم خارج المستوى. تم استخدام طريقة العناصر المحددة فى الدراسة البارامترية لحساب معاملات تركيز الاجهادات. وللتأكد من النموذج المستخدم، تمت مقارنة نتائج الوصلات الغير مقواه مع مثيلاتها الناتجة من المعادلات الوضعية المتاحة. وبعد التأكد من النتائج، تم عمل دراسة بارامترية لتقييم أداء التقويات فى الوصلات ذات القطاعات الدائرية. وقد تم عمل الدراسة البارامترية وذلك بتغيير معاملات هندسة الشكل مثل نسبة سمك القطاعات و نسبة أقطار القطاعات. كذلك تم أعتبار تغير سمك لوح التقوية كنسبة من سمك الضلع الوترى. من النتائج التى تم الحصول عليها، يتضح أن معاملات تركيز الاجهادات فى الوصلات المقواه أقل من مثيلتها فى الوصلات الغير مقواه مما يؤدى الى تحسن أداء هذه الوصلات تحت تأثير أحمال التعب.

Keywords: Stress concentration, CHS Joints, Stiffeners, Fatigue loadings, Finite element method

1. Introduction

Circular Hollow Sections (CHS) are commonly used in offshore structures as structural members due to their inherent properties in minimizing the hydrodynamic force and possessing high torsional rigidity. These members are constantly subjected to the combined action of dynamic forces from waves, wind, and seismic activity. As a result, very high stresses are induced in the tubular joints, especially around the brace/chord intersections.

Currently, there are two methods commonly used in the offshore industry to reinforce tubular joints as a result of alteration and/or addition of loading. The first method makes use of internal stiffeners. Tubular joints reinforced by internal stiffeners have been studied extensively. Callan et al. [1] and Agostoni et al. [2] studied the stress distribution of ring-stiffened tubular joints. Holmes et al. [3], Recho et al. [4], Reynolds and Sharp [5], Munaswamy et al. [6], Chen [7], and Dharmavasan and Aaghaakouchak [8] studied the stress distribution of internally ring-stiffened tubular joints. Internal stiffening is considered the most effective and least costly method to reinforce large diameter tubular joints of offshore structures [9]. It can provide the necessary rigidity and ultimate strength, without using excessively large wall thickness. However, when the structure is in service, inspection and reparation of the

internal stiffeners are difficult. Furthermore, the use of tubes of small diameter also prevents the use of internal stiffeners due to accessibility problems [10].

The second method is to use doubler plates or gusset plates. Reinforcing tubular joints with doubler plates can solve punching shear failure problems due to axial compression. Fung et al. [11] and Choo et al. [12] tested and analyzed tubular joints with doubler plates to calculate the ultimate static strength of the joint under various types of loadings. The results showed that the doubler plate was effective in resisting axial compression, axial tension, inplane and out-of-plane moments. As for the study on the Stress Concentration Factors (SCFs) of welded tubular joints reinforced with the doubler plate, Fung et al. [10] verified this method of reinforcing experimentally. Soh and Soh [13] and Soh et al. [14] presented a numerical study on the stress analysis of doubler plate reinforced tubular joints subjected to axial tension and inplane bending load. Their analysis showed that doubler plate reinforced joints would have less severe fatigue problems than the corresponding unreinforced joints due to axial load under certain conditions.

Other studies were carried out by Soh et al. [15] and Fung et al. [12]. Both the axial compression and out-of-plane bending load were considered in these studies. Results consistent with the previous study were obtained (i.e., doubler plate reinforced joints will not have a more severe fatigue problem than the corresponding unreinforced joints under axial tension and bending while the performance under axial compression can be significantly improved). Berkhout [16] has also presented some numerical SCF results for doubler plate joints.

In this paper, a new method to reinforce tubular joints is investigated. The method depends on using side stiffeners welded to the brace and chord of the joints. Hence to evaluate the performance of the new method, it is important to study the behavior of this stiffened tubular joints under various types of loadings.

Apart from the ultimate capacity, fatigue strength should be considered in the design of tubular joints. Fatigue failure could occur even when the stress level is much lower than the ultimate strength of the material. Hence, the ultimate strength failure criterion is inadequate to handle fatigue problems.

A practical way to deal with fatigue is to relate fatigue failure to the corresponding S-N curves. Hot Spot Stresses (HSS) in conjunction with the appropriate S-N curves are widely used to determine fatigue life in designing offshore structures [17]. Hot spot stress is normally defined as the extrapolated stress at the weld toe, from the stresses within the linear extrapolation region as recommended in the New Guidelines for Fatigue of Hot Spot Stress Connections [18]. Instead of using the principal stresses, the stresses perpendicular to the weld toe are also recommended. The major discontinuity in tubular joints is at the brace/chord intersection where hot spot stresses could occur in these regions.

To generalize the results, the SCF is introduced as a dimensionless ratio of the hot spot stress, σ_{HSS}, to the nominal stress, σ_N, obtained by the simple beam theory, where

$$SCF = \frac{\sigma_{HSS}}{\sigma_N} . \quad (1)$$

Many researchers have established empirical SCF formulae for various types of unstiffened tubular joints. The results are expressed in terms of some nondimensional geometric parameters; the commonly used nondimensional geometric parameters in tubular joint design are:

1. $\alpha = 2L / D$: chord length parameter, indicating the chord beam bending characteristics;
2. $\beta = d / D$: diameter ratio, indicating the compactness of the joints;
3. $\gamma = D / 2T$: the ratio between the diameter and the thickness of the chord, indicating the slenderness ratio of the chord; and
4. $\tau = t / T$: wall thickness ratio, indicating the likelihood that the chord wall will fail before the brace cross section fractures.

Where, L is the length of the chord member, d is the diameter of the brace member, D is the diameter of the chord member, t is the thickness of the brace member, and T is the thickness of the chord member.

Additional parameter related to the stiffened plate welded to the unstiffened joints is the thickness of the stiffened plate, t_s. Fig. 1 shows a typical welded CHS joint reinforced with stiffened plate.

2. Finite-element analysis

In this study, the commercial software package COSMOS/M V. 2.6 [19] is used. Isoparametric thin shell elements with 4-nodes at the corners are adopted in this study. In general, the stress concentration usually occurs near the weld area. Hence, the modelling of weld should have a significant influence on the stress result near the weld area. At the intersection of the brace and the chord and at the intersections at the stiffener and the brace and the chord, the actual thickness and the presence of the weld create a zone of a very complicated three-dimensional stress distribution. So, the finite element mesh is chosen to be quite fine around the area of inclusion and intersections where maximum stresses may occur.

In the analysis, the material properties of the brace, chord, and stiffeners are taken as 210,000 N/mm^2 for modulus of elasticity, E, and 0.30 for Poisson's ratio, ν. The welding material is assumed to have the same material properties as structural steel.

Three basic load cases, namely, axial compression, inplane and out-of-plane bending moments, are considered in the numerical study. For the axial load, only one quarter of the joint is modelled. For inplane and out-of-plane bending, one half of the joint is modelled. Appropriate boundary conditions are assigned along the planes of symmetry. The ends of the chord member are introduced as hinged supports in the finite element model. Fig. 2 shows the typical finite element mesh of the model for the stiffened and unstiffened CHS joint.

3. Verification of the finite element results

The SCFs obtained from the numerical analysis and those obtained from the empirical formulae were used for comparison to verify the suggested finite element model for unstiffened CHS joints. Three load cases were considered (namely, axial compression, inplane and out-of-plane bending moments). The available empirical formulae used in the comparison are those obtained by Gibstein [20], Wordsworth [21], Potvin [22] and Efthymiou [23].

Table 1 lists summary of the empirical SCF formulae for unstiffened tubular T-joints. While table 2 shows the SCFs at the brace and chord for all cases of loadings obtained by the numerical analysis and by empirical formulae. The SCFs at the brace and chord are presented at figs. 3 to 8 for all loadings.

From the results tabulated in table 2 and plotted in figs. 3 to 8, it can be noticed that:

- The empirical formulae have significant differences between each others. This is because that these formulae are based on experimental and numerical results which have different assumptions and approximations.
- In case of axial force, the finite element results look to be within the results of the empirical formulae for chord position. While, for brace position the finite element results tend to be more reliable by increasing the thickness ratio, τ.
- The results of the finite element model are almost close to those of Gibstein formula [20] in case of inplane moment. On the other hand, the finite element results look to be near to those of Wordsworth formula [21] in case of out-of-plane moment.

4. Parametric study

In this study, finite element analyses are conducted for a wide range of stiffened and unstiffened CHS joints to calculate the SCFs of these joints. Three basic load cases namely, axial compression, inplane and out-of-plane bending moments, are considered in the study to evaluate the performance of stiffeners on the performance of CHS joints. For each load case, two of the geometrical parameters of the joints are studied. The first parameter is the diameter ratio between the brace and the chord member, β, and is taken equals 0.3, 0.5 and 0.7. For each β the thickness ratio, τ, between the brace and chord member is changed and is taken equals 0.25, 0.50 and 1.00. Additional parameter in case of stiffened joints namely the thickness of the stiffener plate, t_s, is introduced as a ratio from the

chord wall thickness, T, ($\psi=t_s/T$). This ratio is varied and is taken equals 0.25, 0.50 and 1.00.

For all the analyzed joints, the length of the chord is taken equals 350 cm (i.e. α=14), the slenderness ratio of the chord equals 12 (i.e. γ=12), the height of the brace equals 150 cm, and the height of the stiffener plate equals 20 cm with slope 1:1.

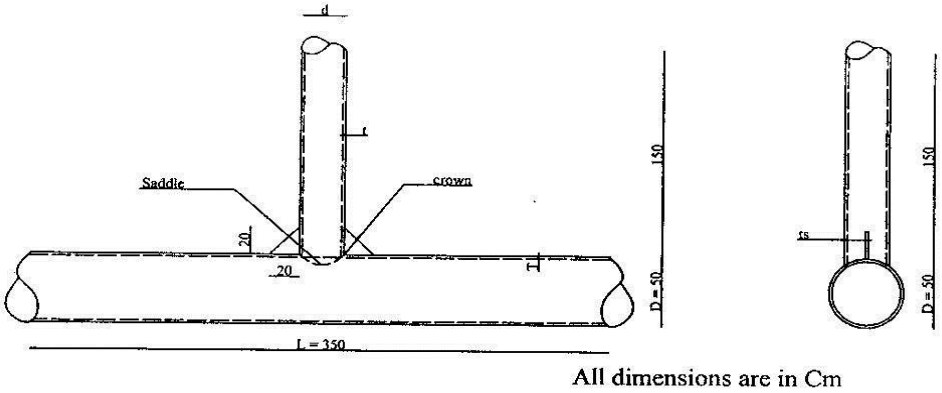

Fig. 1. Typical welded CHS T-joint reinforced by stiffened plate.

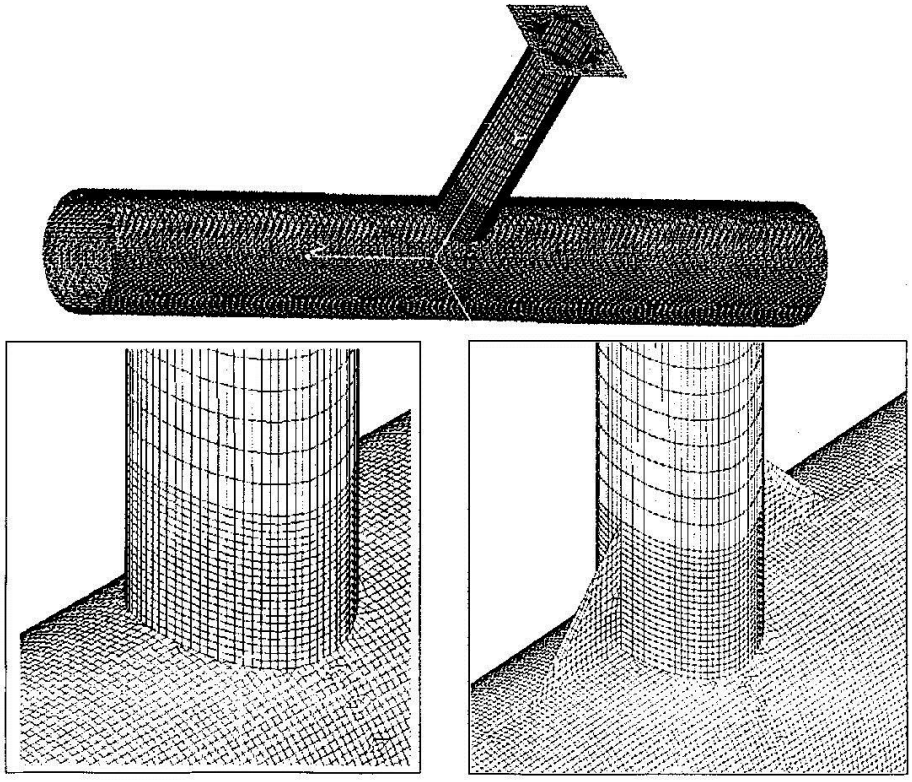

Fig. 2. Finite element mesh of the analyzed un-stiffened and stiffened CHS joints.

Table 1
summary of the empirical SCF formulae for unstiffened tubular joints

Formula by	Load application	SCF formula	Validity range
Gibstein [20]	Axial force	Chord: $SCF=[1.5-3.88(\beta-0.47)^2].\gamma^{0.87}.(\tau)^{1.37}.(\alpha/2)^{0.06}.\sin^{1.69}\theta$ Brace: $SCF=[1.09-1.93(\beta-0.5)^2].\gamma^{0.76}.(\tau)^{0.57}.(\alpha/2)^{0.12}.\sin^{1.94}\theta$	$0.3\le\beta\le0.9$ $10\le\gamma\le30$ $0.4\le\tau\le1.0$ $3.5\le\alpha/2\le8.0$
	Inplane moment	Chord: $SCF=[1.65-1.1(\beta-0.42)^2].\gamma^{0.38}.(\tau)^{1.05}.\sin^{0.57}\theta$ Brace: $SCF=[0.95-0.65(\beta-0.41)^2].\gamma^{0.39}.(\tau)^{0.29}.\sin^{0.21}\theta$	
	Out-of-plane moment	Chord: $SCF=[1.01-3.36(\beta-0.64)^2].\gamma^{0.95}.(\tau)^{1.18}.\sin^{1.56}\theta$ Brace: $SCF=[0.76-1.92(\beta-0.72)^2].\gamma^{0.89}.(\tau)^{0.47}.\sin^{2.03}\theta$	
Wordsworth [21]	Axial force	Chord: $SCF=\gamma.\tau.\beta.(6.78-6.42\beta^{0.5}).\sin^{(1.7+0.7\beta^3)}\theta$ Brace: $SCF=1+0.63\ SCF_{chord}$	$0.13\le\beta\le1.0$ $12\le\gamma\le32$ $0.25\le\tau\le1.0$ $8\le\alpha\le40$
	Inplane moment	Chord: $SCF=0.75\gamma^{0.6}.\tau^{0.8}.(1.6\beta^{0.25}-0.7\beta^2).\sin^{(1.5-1.6\beta)}\theta$ Brace: $SCF=1+0.63\ SCF_{chord}$	
	Out-of-plane moment	Chord: $SCF=\gamma.\tau.\beta.(1.56-1.46\beta^5).\sin^{\beta^2(15-14.4\beta)}\theta$ Brace: $SCF=1+0.63\ SCF_{chord}$	
Potvin [22]	Axial force	Chord: $SCF=1.981.\gamma^{0.808}.(\tau)^{1.333}.(\alpha)^{0.057}.\ e^{-1.2\beta^3}\sin^{1.694}\theta$ Brace: $SCF=3.751.\gamma^{0.55}.(\tau).(\alpha)^{0.12}.\ e^{-1.35\beta^3}\sin^{1.94}\theta$	$0.3\le\beta\le1.0$ $8\le\gamma\le33$ $0.2\le\tau\le0.8$ $7\le\alpha\le40$
	Inplane moment	Chord: $SCF=0.702.\gamma^{0.6}.(\tau)^{0.86}.(\beta)^{-0.04}.\sin^{0.57}\theta$ Brace: $SCF=1.301.\gamma^{0.23}.(\tau)^{0.38}.(\beta)^{-0.38}.\sin^{0.21}\theta$	
	Out-of-plane moment	Chord: $SCF=1.024.\beta^{0.787}.\gamma^{1.014}.(\tau)^{0.889}.\sin^{1.557}\theta$	$0.3\le\beta\le0.55$
		$SCF=0.462.\beta^{-0.619}.\gamma^{1.014}.(\tau)^{0.889}.\sin^{1.557}\theta$	$0.55\le\beta\le0.75$
		Brace: $SCF=1.552.\beta^{0.801}.\gamma^{0.852}.(\tau)^{0.543}.\sin^{2.033}\theta$	$0.3\le\beta\le0.55$
		$SCF=0.796.\beta^{-0.281}.\gamma^{0.852}.(\tau)^{0.543}.\sin^{2.033}\theta$	$0.55\le\beta\le0.75$
Efthymiou [23]	Axial force	Chord: $SCF=\gamma.(\tau)^{1.1}[1.11-3(\beta-0.52)^2]$ Brace: $SCF=1.3+\gamma.(\tau)^{0.52}.[0.187-1.25\beta^{1.1}(\beta-0.96)]$	$0.3\le\beta\le1.0$ $8\le\gamma\le33$ $0.2\le\tau\le1.0$

Table 2
SCFs calculated from the empirical formulae and the finite element model for un-stiffened CHS T-joints
a) case of axial force

Position	β	τ	(SCF)ax				
			Gibstein formula	Wordsworth formula	Potvin Formula	Efthymiou formula	F.E results
Chord	0.30	0.25	2.03	2.94	2.63	2.52	2.45
		0.50	5.24	5.87	6.60	5.40	5.91
		1.00	13.55	11.75	16.60	11.58	14.52
	0.50	0.25	2.19	3.36	2.34	2.90	2.52
		0.50	5.65	6.72	5.87	6.21	6.26
		1.00	14.61	13.44	14.76	13.31	15.62
	0.70	0.25	1.89	2.96	1.80	2.65	2.39
		0.50	4.89	5.92	4.52	5.67	6.04
		1.00	12.64	11.83	11.36	12.15	15.77
Brace	0.30	0.25	3.84	2.85	4.87	3.67	1.76
		0.50	5.70	4.70	9.74	4.70	3.75
		1.00	8.45	8.40	19.47	6.18	7.25
	0.50	0.25	4.13	3.12	4.26	3.96	1.56
		0.50	6.13	5.23	8.53	5.11	3.39
		1.00	9.10	9.47	17.06	6.76	6.83
	0.70	0.25	3.84	2.86	3.18	3.67	1.50
		0.50	5.70	4.73	6.35	4.70	3.36
		1.00	8.45	8.45	12.71	6.18	6.99

b) Case of inplane moment

Position	β	τ	(SCF)ip			
			Gibstein formula	Wordsworth formula	Potvin formula	F.E results
Chord	0.30	0.25	0.98	1.23	0.99	1.09
		0.50	2.03	2.14	1.80	2.22
		1.00	4.20	3.73	3.27	4.68
	0.50	0.25	0.99	1.29	0.97	1.07
		0.50	2.04	2.24	1.77	2.08
		1.00	4.22	3.90	3.21	4.27
	0.70	0.25	0.94	1.23	0.96	1.06
		0.50	1.94	2.14	1.74	1.95
		1.00	4.02	3.73	3.16	3.89
Brace	0.30	0.25	1.66	1.78	2.15	0.88
		0.50	2.03	2.35	2.80	1.58
		1.00	2.48	3.35	3.64	2.57
	0.50	0.25	1.67	1.81	1.77	0.84
		0.50	2.04	2.41	2.30	1.45
		1.00	2.49	3.46	3.00	2.38
	0.70	0.25	1.58	1.78	1.56	0.76
		0.50	1.93	2.35	2.03	1.25
		1.00	2.36	3.35	2.64	2.15

c) case of out-of-plane moment

Position	β	τ	(SCF)op			
			Gibstein formula	Wordsworth formula	Potvin Formula	F.E results
Chord	0.30	0.25	1.28	1.44	1.44	1.66
		0.50	2.91	2.87	2.66	3.49
		1.00	6.59	5.75	4.93	7.67
	0.50	0.25	1.95	2.35	2.15	2.35
		0.50	4.42	4.69	3.98	5.10
		1.00	10.01	9.38	7.37	11.37
	0.70	0.25	2.06	2.95	2.09	2.49
		0.50	4.67	5.91	3.87	5.66
		1.00	10.58	11.82	7.16	13.32
Brace	0.30	0.25	2.00	1.91	2.32	1.06
		0.50	2.78	2.81	3.37	2.02
		1.00	3.85	4.62	4.92	3.57
	0.50	0.25	3.17	2.48	3.49	1.29
		0.50	4.40	3.96	5.08	2.54
		1.00	6.09	6.91	7.40	4.57
	0.70	0.25	3.61	2.86	3.44	1.37
		0.50	5.00	4.72	5.02	2.88
		1.00	6.93	8.44	7.31	5.50

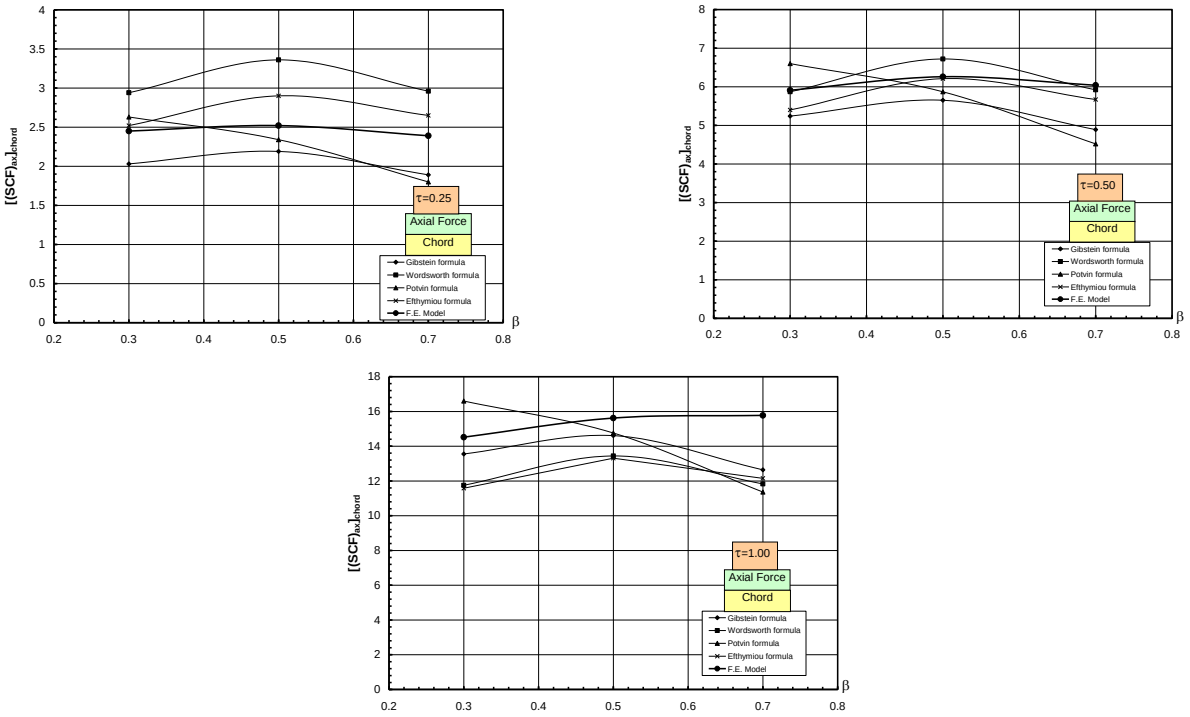

Fig. 3. Comparison between the SCFs of the finite element model and those of empirical formulae at chord for different τ ratios (case of axial force).

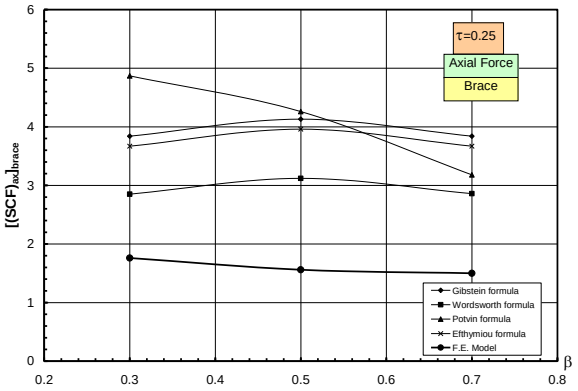

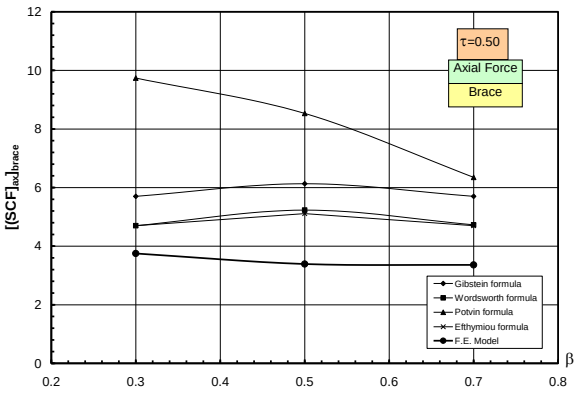

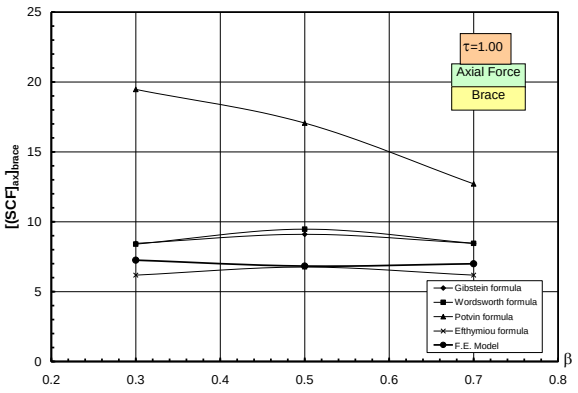

Fig. 4. Comparison between the SCFs of the finite element model and those of empirical formulae at brace for different τ ratios (case of axial force).

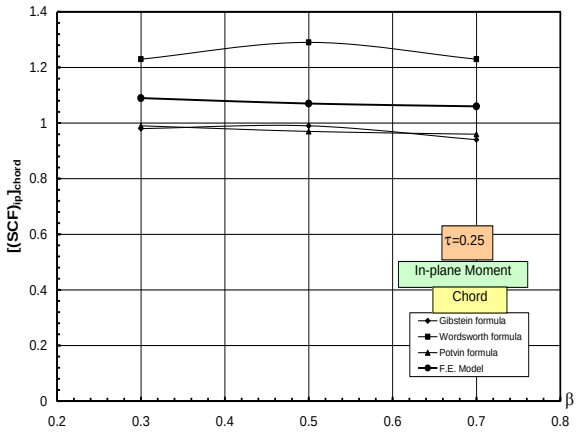

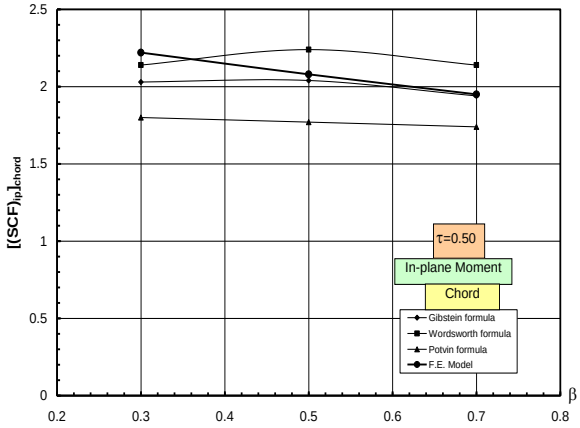

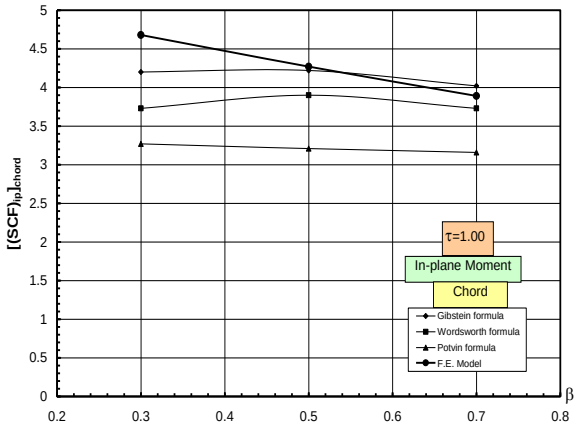

Fig. 5. Comparison between the SCFs of the finite element model and those of empirical formulae at chord for different τ ratios (case of inplane moment).

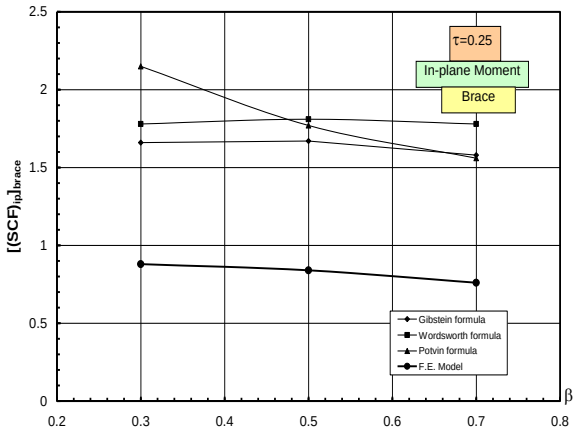

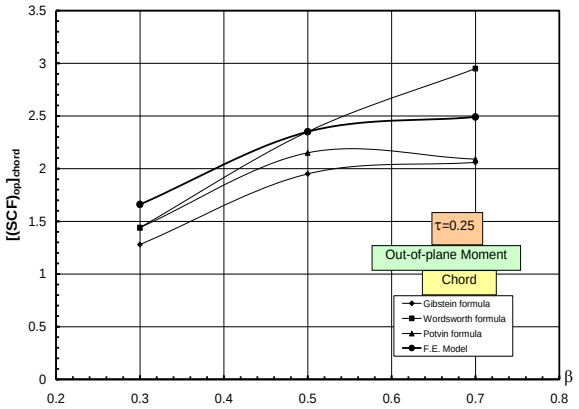

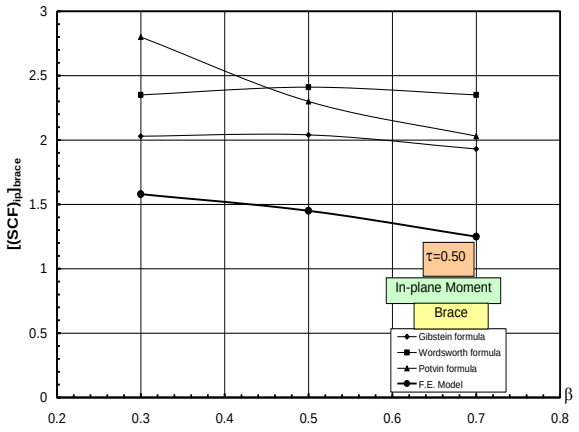

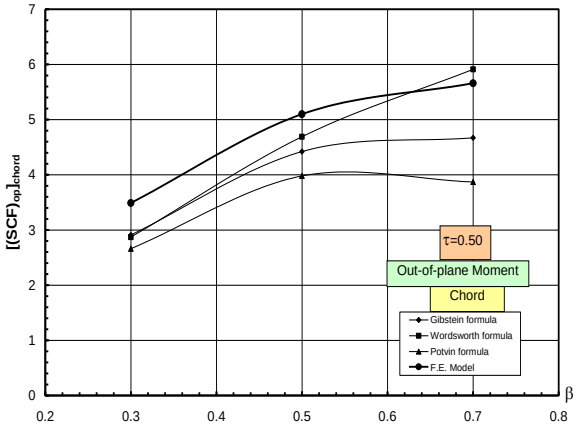

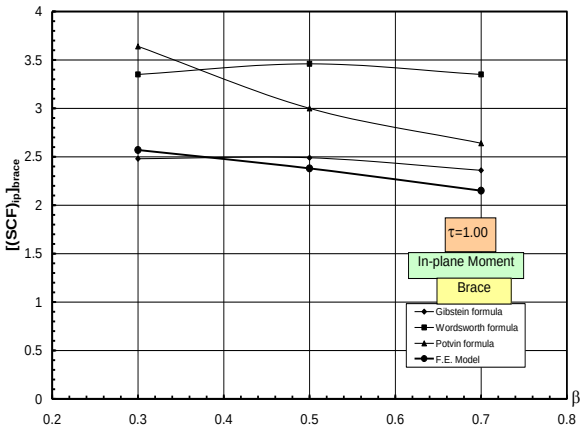

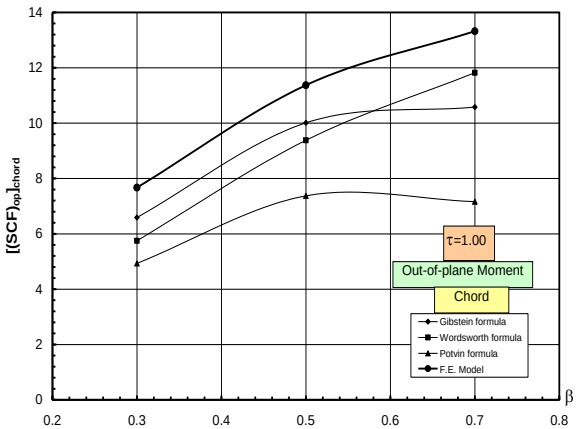

Fig. 6. Comparison between the SCFs of the finite element model and those of empirical formulae at brace for different τ ratios (case of inplane moment).

Fig. 7. Comparison between the SCFs of the finite element model and those of empirical formulae at chord for different τ ratios (case of out-of-plane moment).

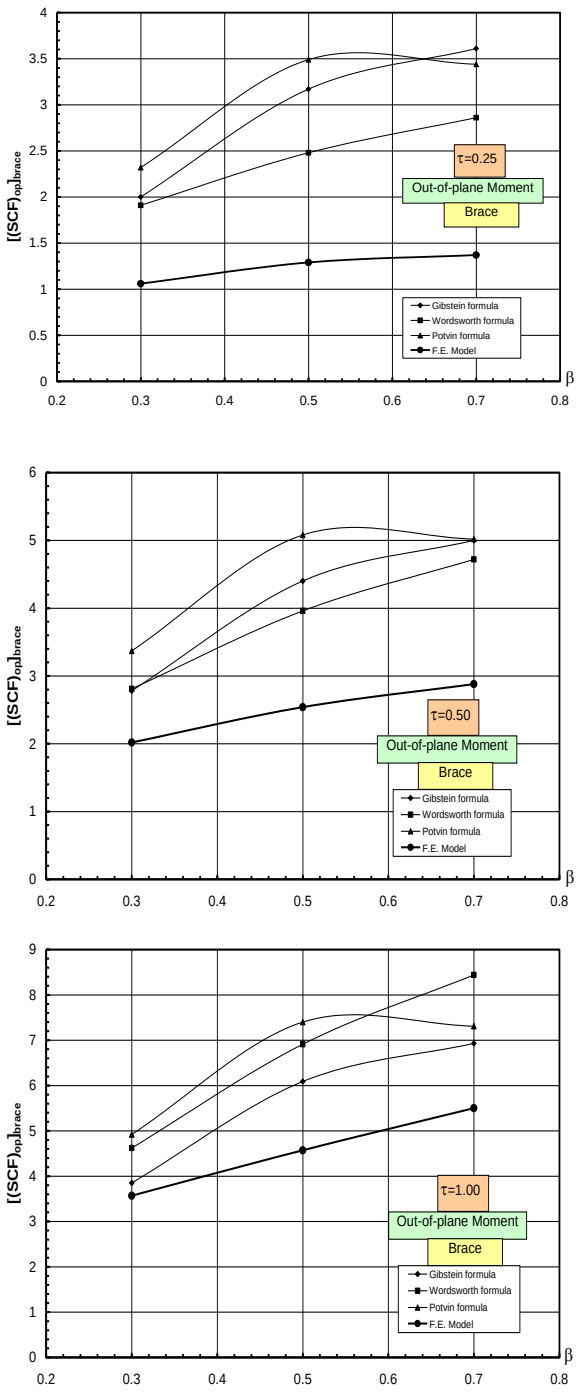

Fig. 8. Comparison between the SCFs of the finite element model and those of empirical formulae at brace for different τ ratios (case of out-of-plane moment).

The results of the parametric study are listed in table 3 for all the analyzed joints under different loading conditions. Also, the results are plotted in figs. 9 to 13 for different geometrical parameters at different joint locations in case of axial force, inplane moment, out-of-plane moment, axial force with inplane moment and axial force with inplane and out-of-plane moments. The plotted results are in the form of a ratio between the SCF for stiffened joints and the SCF for unstiffened joints. In the following subsections the obtained numerical results are discussed.

5. Discussion of results

5.1. Influence of width ratio, β, on stress concentration factors

Table 3 shows that under axial loading, an increase of β results in a slightly increase of SCFs at the chord locations, meanwhile a slightly decrease of SCFs at the brace locations occur by increasing the β value. The β value does not have much effect on the stresses in case of CHS joints reinforced by stiffened plate. Under inplane moment, on the brace and on the chord, the increase of β value decreases the SCFs. For out-of-plane moment, the SCF values consistently increase with increasing the β value for both the chord and the brace.

5.2. Influence of wall thickness ratio, τ, on stress concentration factors

From table 3, it can be noticed that for axial loading, an increase of τ ratio increases the SCF ranges. The changes of the range are more significant on the SCFs at the chord than the SCFs at the brace. This implies that the influence of τ on SCFs at the chord is more significant than the SCFs at the brace. The same phenomena occur for inplane and out-of-plane moments.

Table 3
Stress concentration factors from finite element analyses for all the analyzed joints
a) chord locations

Position	β	τ	SCF for axial force				SCF for inplane moment				SCF for out-of-plane moment			
			No stiff.	ψ=0.25	ψ=0.50	ψ=1.00	no stiff.	ψ=0.25	ψ=0.50	ψ=1.00	No stiff.	ψ=0.25	ψ=0.50	ψ=1.00
chord-crown	0.30	0.25	1.37	0.63	0.63	0.62	1.09	0.33	0.33	0.35	0.02	0.02	0.01	0.00
		0.50	3.54	0.60	0.50	0.45	2.22	0.30	0.26	0.24	0.05	0.03	0.00	-0.03
		1.00	5.47	1.46	1.08	0.86	4.68	0.40	0.26	0.19	0.12	0.11	0.05	-0.02
	0.50	0.25	1.29	0.81	0.83	0.84	1.07	0.61	0.63	0.65	0.04	0.03	0.02	0.00
		0.50	2.14	0.86	0.84	0.84	2.08	0.61	0.58	0.57	0.06	0.05	0.01	0.02
		1.00	4.31	1.39	1.17	1.06	4.27	0.76	0.58	0.50	0.10	0.10	0.04	-0.02
	0.70	0.25	1.41	1.15	1.20	1.23	1.06	0.78	0.81	0.84	0.07	0.05	0.11	0.03
		0.50	2.46	1.42	1.43	1.45	1.95	0.89	0.87	0.88	0.10	0.07	0.04	0.02
		1.00	4.90	1.84	1.67	1.58	3.89	1.03	0.86	0.78	0.15	0.12	0.06	0.01
chord-saddle	0.30	0.25	2.45	2.56	2.56	2.55	0.24	0.10	0.10	0.10	1.66	1.64	1.62	1.58
		0.50	5.91	5.68	5.65	5.62	0.47	0.14	0.12	0.11	3.49	3.47	3.43	3.36
		1.00	14.52	13.21	12.99	12.89	0.89	0.26	0.23	0.21	7.67	7.65	7.58	7.46
	0.50	0.25	2.52	2.65	2.65	2.65	0.14	0.13	0.13	0.13	2.35	2.35	2.35	2.34
		0.50	6.26	6.37	6.36	6.36	0.35	0.26	0.25	0.24	5.10	5.11	5.09	5.08
		1.00	15.62	15.37	15.29	15.25	0.93	0.60	0.56	0.53	11.37	11.39	11.37	11.34
	0.70	0.25	2.39	2.41	2.41	2.41	0.35	0.21	0.21	0.21	2.49	2.49	2.49	2.49
		0.50	6.04	6.12	6.14	6.14	0.66	0.41	0.40	0.40	5.66	5.66	5.67	5.67
		1.00	15.77	15.76	15.78	15.78	1.18	0.79	0.77	0.76	13.32	13.33	13.32	13.32

b) brace locations

Position	β	τ	SCF for axial force				SCF for inplane moment				SCF for out-of-plane moment			
			No stiff.	ψ=0.25	ψ=0.50	ψ=1.00	no stiff.	ψ=0.25	ψ=0.50	ψ=1.00	no stiff.	ψ=0.25	ψ=0.50	ψ=1.00
brace-crown	0.30	0.25	1.54	0.93	0.93	0.94	0.88	0.36	0.37	0.38	0.08	0.06	0.04	0.02
		0.50	2.23	1.07	1.01	0.97	1.58	0.38	0.35	0.34	0.14	0.06	-0.01	-0.08
		1.00	3.05	1.32	1.14	1.04	2.57	0.48	0.40	0.36	0.21	-0.01	-0.19	-0.32
	0.50	0.25	1.03	0.59	0.60	0.61	0.84	0.57	0.59	0.62	0.04	0.01	-0.02	-0.05
		0.50	1.33	0.53	0.50	0.49	1.45	0.62	0.60	0.59	0.02	-0.09	-0.16	-0.23
		1.00	1.91	0.65	0.54	0.49	2.38	0.75	0.65	0.60	-0.13	-0.37	-0.53	-0.65
	0.70	0.25	0.83	0.57	0.59	0.60	0.76	0.63	0.67	0.70	0.00	-0.04	0.09	-0.10
		0.50	1.14	0.48	0.45	0.45	1.25	0.73	0.72	0.73	-0.09	-0.18	-0.24	-0.30
		1.00	1.90	0.49	0.37	0.31	2.15	0.86	0.77	0.72	-0.29	-0.46	-0.58	-0.66
brace-saddle	0.30	0.25	1.76	1.85	1.85	1.84	0.14	0.01	0.01	0.01	1.06	1.05	1.03	1.00
		0.50	3.75	3.60	3.57	3.56	0.07	0.03	0.03	0.02	2.02	2.01	1.98	1.94
		1.00	7.25	6.51	6.39	6.33	0.28	0.10	0.09	0.08	3.57	3.56	3.53	3.47
	0.50	0.25	1.56	1.61	1.61	1.61	0.09	0.08	0.08	0.08	1.29	1.29	1.29	1.28
		0.50	3.39	3.44	3.43	3.43	0.17	0.12	0.11	0.11	2.54	2.54	2.53	2.53
		1.00	6.83	6.68	6.63	6.61	0.27	0.15	0.14	0.13	4.57	4.56	4.56	4.55
	0.70	0.25	1.50	1.50	1.49	1.49	0.16	0.26	0.26	0.26	1.37	1.37	1.37	1.37
		0.50	3.36	3.40	3.41	3.41	0.37	0.51	0.51	0.51	2.88	2.88	2.88	2.88
		1.00	6.99	6.99	6.99	6.99	0.86	1.00	0.98	0.96	5.50	5.51	5.50	5.50

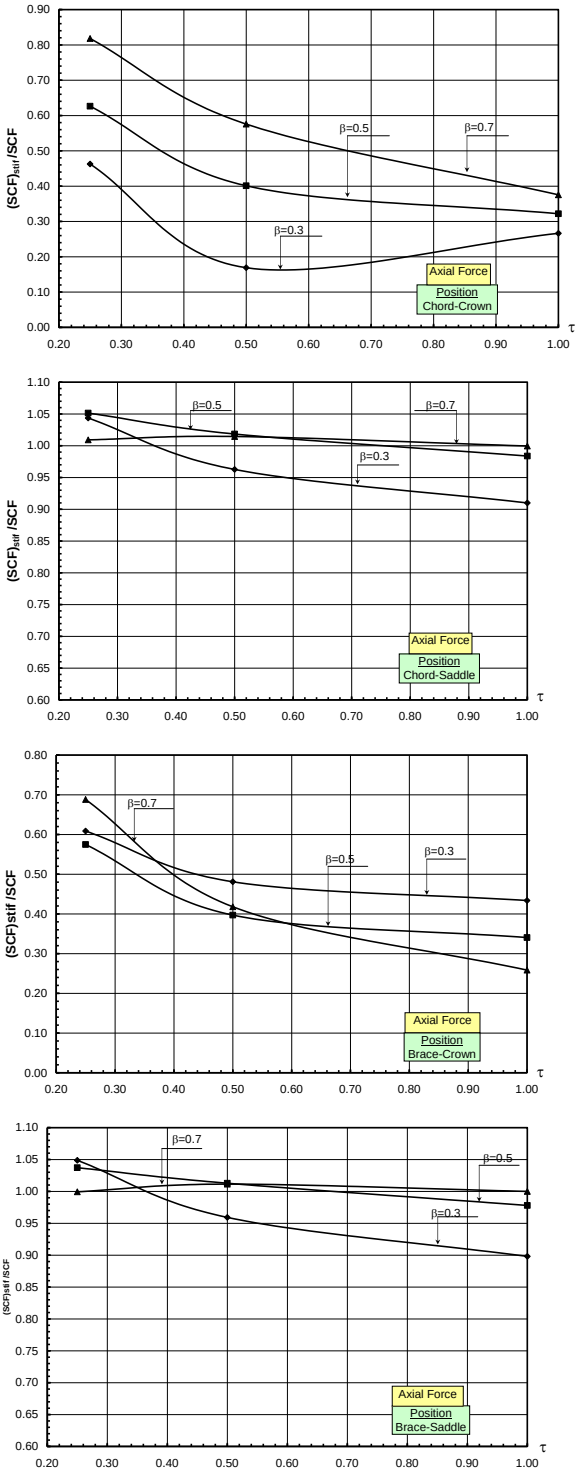

Fig. 9. Effect of the presence of stiffener on the SCFs at different joint locations for different geometrical parameters (case of axial force).

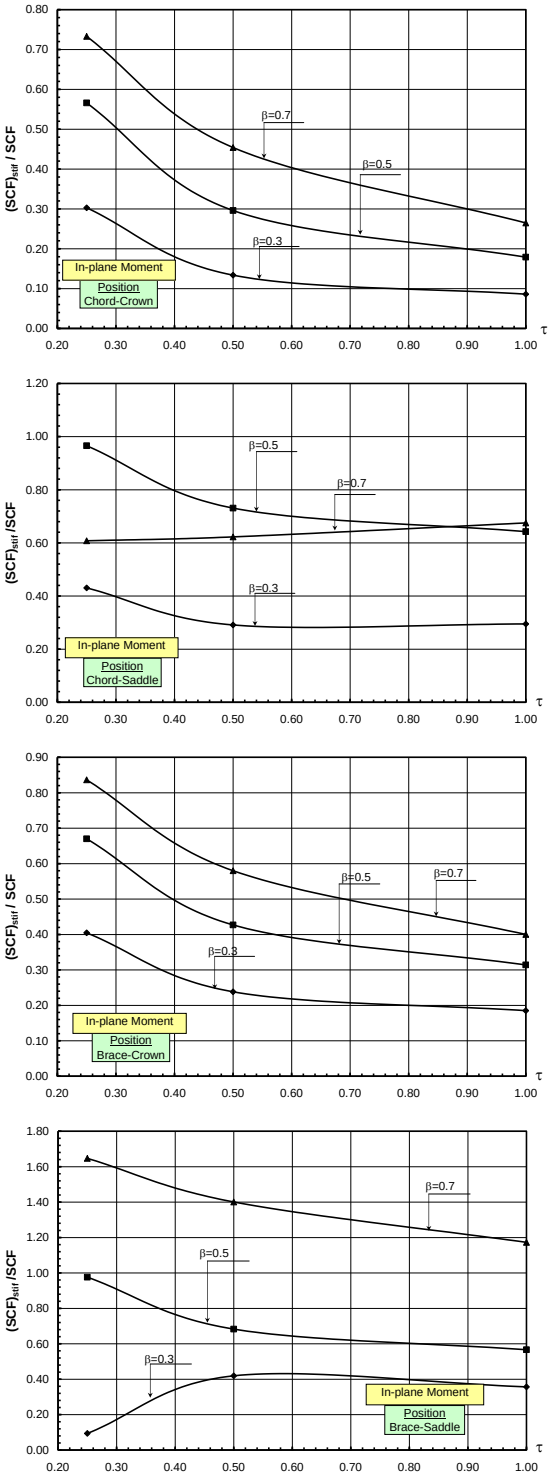

Fig.10. Effect of the presence of stiffener on the SCFs at different joint locations for different geometrical parameters (case of inplane moment).

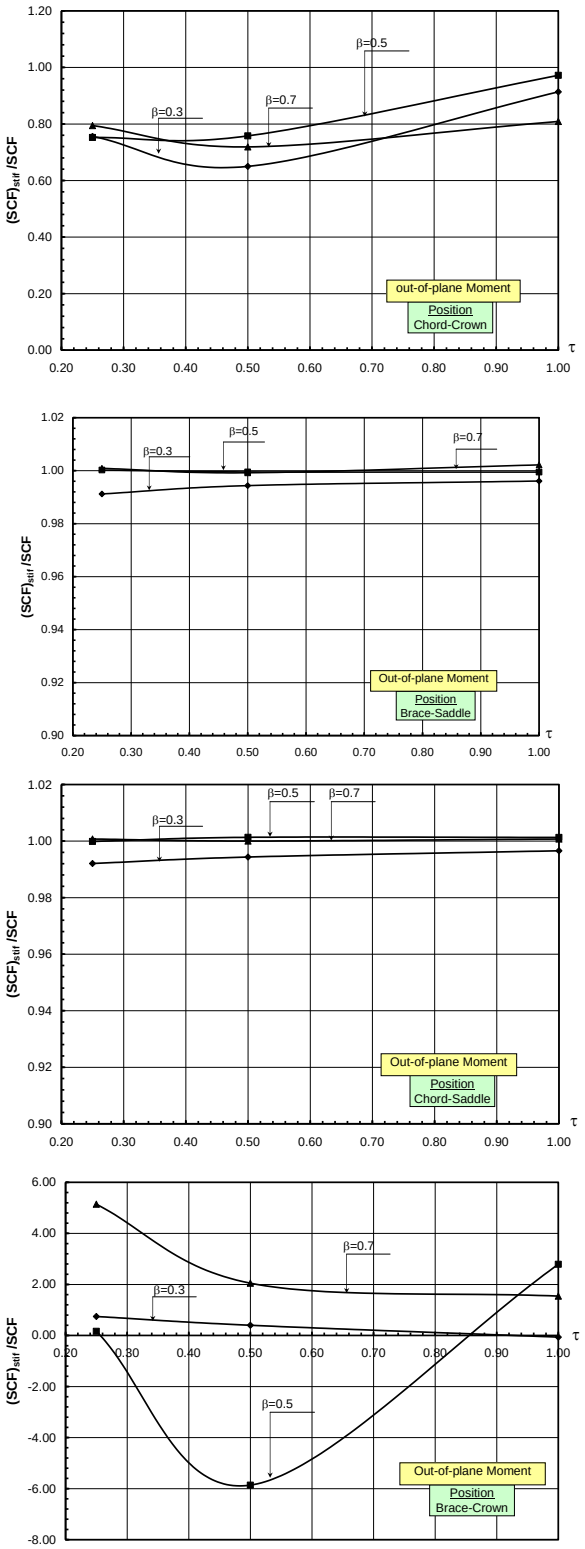

Fig. 11. Effect of the presence of stiffener on the SCFs at different joint locations for different geometrical parameters (case of out-of-plane moment).

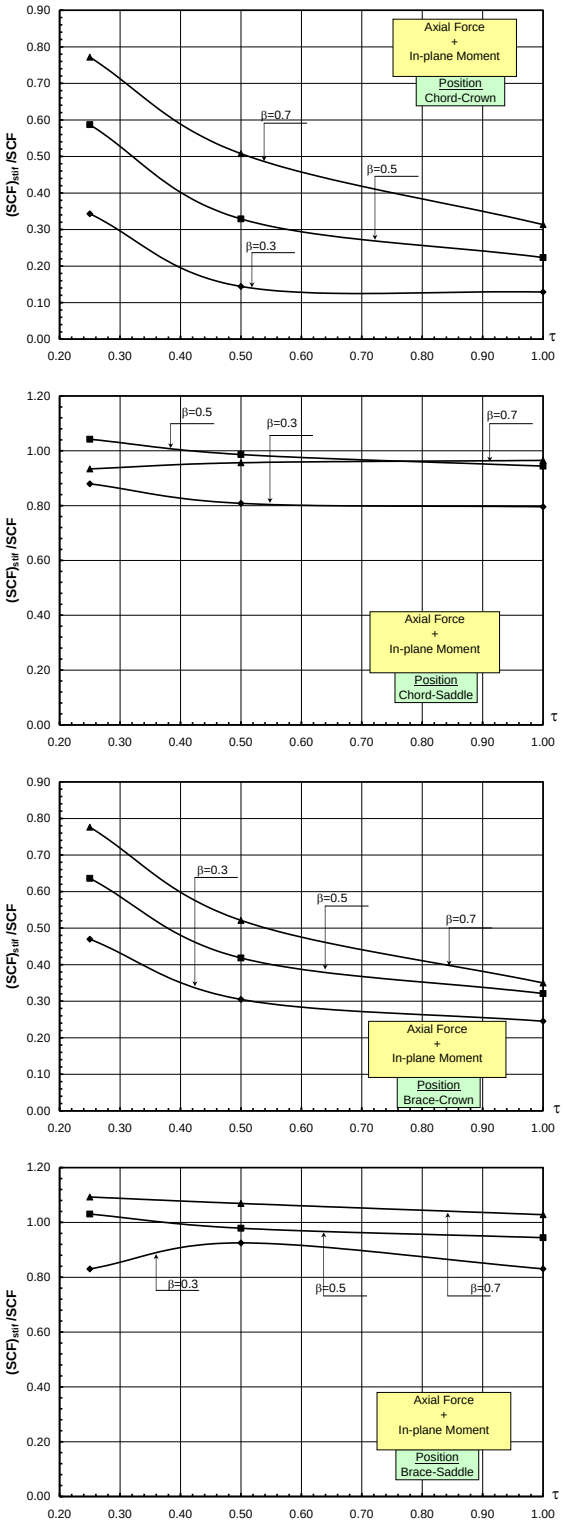

Fig. 12. Effect of the presence of stiffener on the SCFs at different joint locations for different geometrical parameters (case of combined axial force and inplane moment).

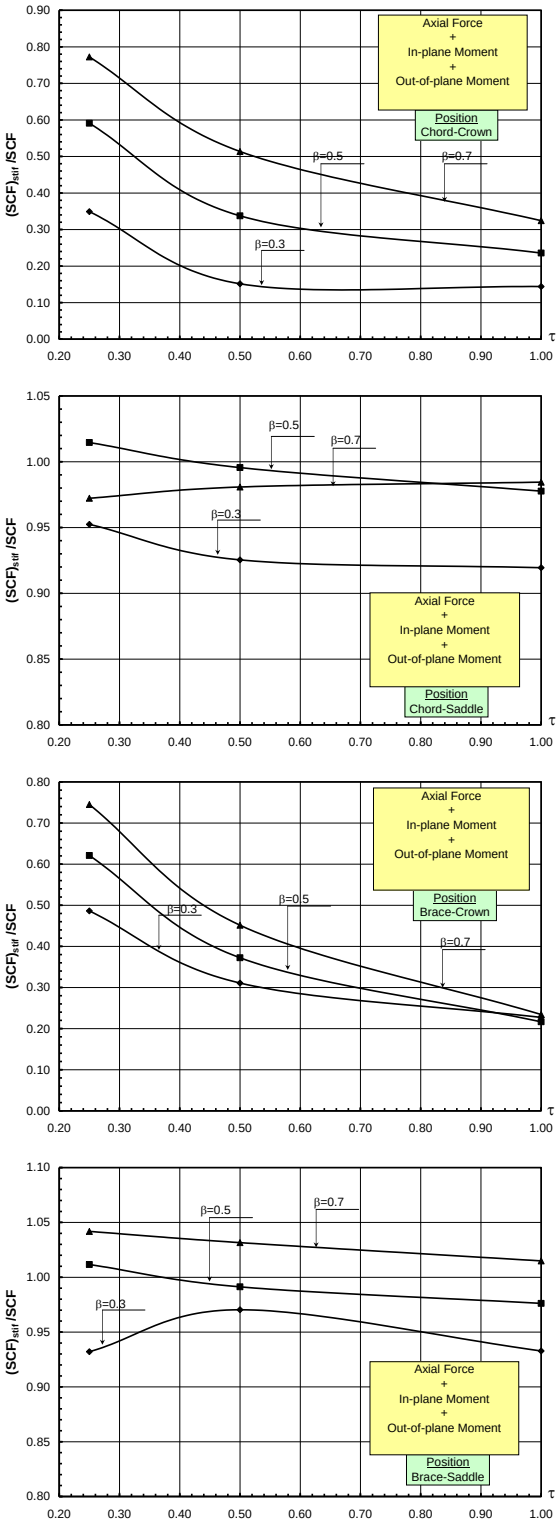

Fig. 13. Effect of the presence of stiffener on the SCFs at different joint locations for different geometrical parameters (case of combined axial force, inplane and out-of-plane moments).

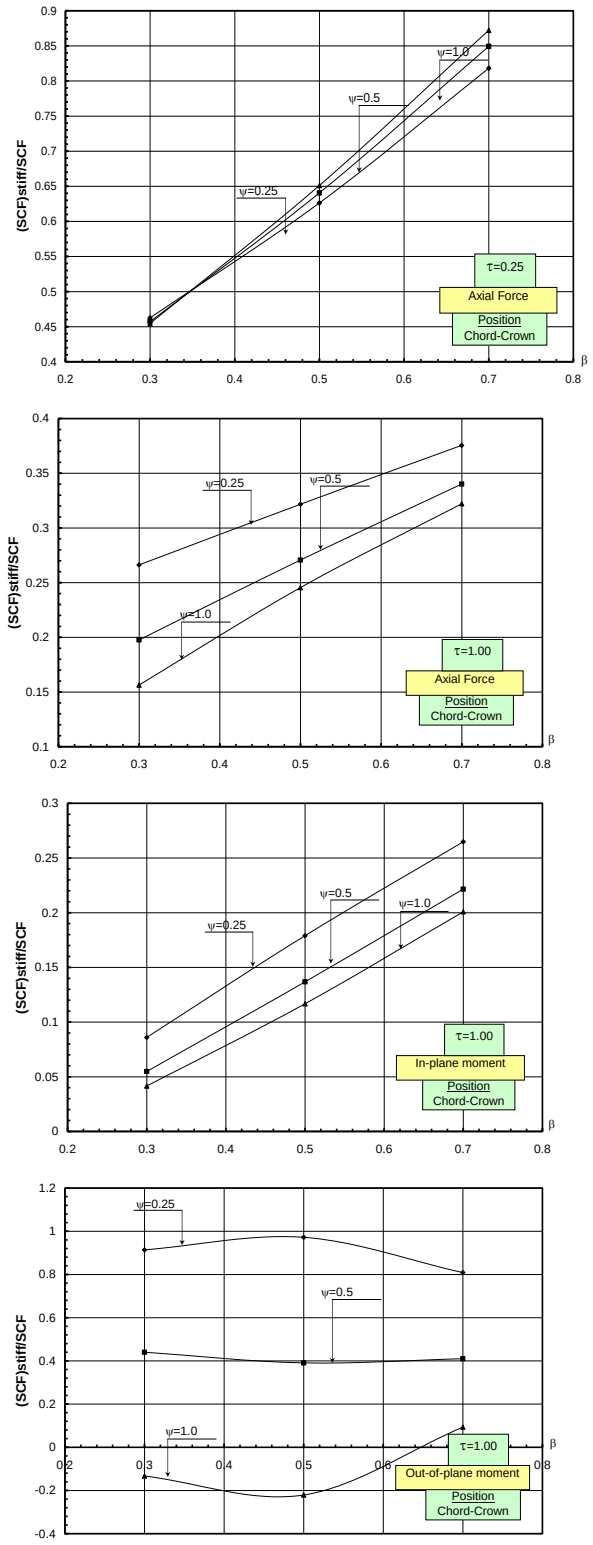

Fig. 14. Effect of the thickness of the stiffened plate as a ratio from the thickness of the chord member, ψ, on the SCFs at chord-crown location.

5.3. Influence of reinforcing CHS joints by stiffened plates

To study the contribution of the stiffened plate to SCF reduction, a series of reinforced T-joints was analyzed numerically for similar types of loading. The modelling technique adopted was exactly the same as discussed earlier, but with the stiffened plates. The geometry ranges considered were also the same: i.e. $0.3 \le \beta \le 0.7$, $0.25 \le \tau \le 1.00$, with $\gamma=12$, and $\alpha=14$. The results are shown in figs. 9 to 13.

Under axial loading, fig. 9 shows that stiffened plate reinforcement gives a very significant reduction in the SCF values at the brace-crown and chord-crown. However, no significant reduction is observed at the brace-saddle and chord-saddle. This is because the stiffened plate is located at the crown of the joint. The same effect of the stiffened plates on the SCFs is observed in case of inplane moment see fig. 10.

For out-of-plane moment, as shown in fig. 11, the SCF reduction for the stiffened plate reinforced T-joints is insignificant compared to the SCF reduction for inplane moment. This is because the stiffened plates are located at the crown while the peak stresses in case of out-of-plane moment occur at the saddle.

Figs. 12 and 13 show the SCF reduction in case of combined axial force and inplane moment and in case of combined axial force and inplane and out-of-plane moments, respectively. In these cases, the same conclusions are observed.

From the comparisons, it is clear that a consistent reduction of SCF for stiffened plate reinforced tubular joints can be achieved. The reduction in SCF values at the crown for chord and brace is significant, especially under axial loading and inplane moment. Generally, the SCFs for the stiffened CHS joints are significantly lower than the SCFs at the unreinforced CHS joints.

5.4. Influence of stiffened plate thickness, t_s, on stress concentration factors

To study the influence of the thickness of the stiffened plate, t_s, the SCFs for various load cases at critical locations considered are listed in Table 3 with $\psi=t_s/T$ = 0.25, 0.5, and 1.0.

Fig. 14 indicates that for all stiffened joints analyzed, it is noticed that the influence of the thickness of the stiffened plate tends to be the same for all load cases at different locations in chord and brace. It is noticed that by increasing τ ratio the effect of the thickness of the stiffened plate on the reduction of SCFs increases.

6. Conclusions

In this paper, the SCFs of stiffened plate reinforced tubular T-joints are presented. Empirical formulae conducted by several researchers were used to verify the finite element modelling techniques. A numerical parametric study was conducted to study the influence of some geometric parameters and to study the performance of CHS joints reinforced by stiffened plates. The results obtained, show that the stiffened plates can be used as a type of reinforcement to reduce the stress concentration of the joints. In this case, the hot spot stresses locations are changed from the area of intersection to the brace and the chord members which enable the joint to sustain more number of cycles (more life time) under fatigue loadings than the unreinforced joints.

References

[1] M. Callan, A. Wordsworth, I. Livett, R. Boudreaux, F. and Huebsch, "BP Magnus Platform Internally Stiffened Bracing Node Studies," Proc., 13th Annual Offshore Technol. Conf., OTC4109, Houston, pp. 397- 409 (1981).

[2] A. Agostoni, V. Tella, E. Gnone, and G. Sebastiani, "TSG-integrated storage platform for early production in the North Sea." Proc., 12th Annual Offshore Tech. Conf., OTC 3880, Houston, pp. 245-260 (1980).

[3] R. Holmes, G. Brown, and J. Kerr, "Internally Ring Stiffened Tubular Joints-Salvation or Structural Liability," Proc., 3rd Int. Symp. on Integrity of Offshore Structures, Univ. of Glasgow, Scotland (1987).

[4] N. Recho, C. Andreau, E. Bouet, and J. Palamas, "Evaluation of Stress Concentration Factors in Ring-Stiffened Tubular Joints," Steel in marine structures: Proc., 3rd Int. ECSC Offshore Conf. on Steel in Marine Structures (SIMS' 87), Delft, The Netherlands (1987).

[5] A. Reynolds, and J. Sharp, "Fatigue Performance Comparison of Simple, Overlapped and Stiffened Welded Tubular Joints," Proc., 3rd Int. Symp. on Integrity of Offshore Structures, Univ. of Glasgow, Scotland (1987).

[6] K. Munaswamy, A. Swamidas, R. Hopkins, C. Monahan, O. and Vosikovsky, "Experimental Study on Fatigue of Stiffened Tubular T Joints," Proc., 8th Int. Conf. on Offshore Mechanics and Arctic Eng., Hague, The Netherlands, pp. 375-382 (1989).

[7] B. Chen, "Review of Studies in China on Stress Analysis of Ring Stiffened Tubular Joints for Offshore Structures," Proc., 9th Int. Conf. on Offshore Mechanics and Arctic Eng., III-(A), pp. 313-319 (1990).

[8] S. Dharmavasan, and A. Aaghaakouchak, "Estimation of Stress Concentration Factors in a Stiffened Tubular Joint Using a Shear Flow Model," Proc., 11th Int. Conf. on Offshore Mechanics and Arctic Eng., III(B), pp. 585-592 (1992).

[9] Underground Engineering Group. (UEG) Design of Tubular Joints for Offshore Structures, UEG, London, U.K. (1985).

[10] T. Fung, C. Soh, T. Chan, and Erni. "Stress Concentration Factors of Doubler Plate Reinforced Tubular T-Joints," ASCE, 128 (11), pp. 1399-1412 (2002).

[11] T. Fung, T. Chan, C. and Soh, "Ultimate Capacity of Doubler Plate Reinforced Tubular Joints," ASCE, 125 (8) pp. 891–899 (1999).

[12] Y. Choo, B. Li, van der G. Vegte, N. Zettlemoyer, and J. Liew, "Static Strength of T Joints Reinforced with Doubler or Collar Plates," Proc., 8th Int. Symp. on Tubular Structures, Balkema, Rotterdam, The Netherlands, pp. 139-146 (1998).

[13] A. Soh, and C. Soh, "Hot Spot Stresses of Tubular Joints Subjected to Combined Loadings," ASCE, 119 (2) pp. 654-661(1993).

[14] A. Soh, C. Soh, and K. Hoon, "Stress Analysis of Reinforced Tubular Joints Subjected to Different Load Types," Proc., Inst. of Civil Engineers-Structures and Buildings, Vol. 104 pp. 257-266 (1994).

[15] C. Soh, T. Fung, and T. Chan, "Analysis of T tubular joints reinforced with doubler plates," Structures in the new millennium, Balkema, Rotterdam, the Netherlands, pp. 319-323 (1997).

[16] K. Berkhout, "Numerical SCF analysis of collar and doubler plate joints," Tubular Structures IX, Proc., 9th Int. Symp. and Euro Conf. on Tubular Structures, Dusseldorf, Germany, Balkema, Rotterdam, The Netherlands (2001).

[17] American Petroleum Institute (API). Recommended Practice for Planning, Designing, and Constructing Fixed Offshore Structures, 20th Ed., API, Washington D.C. (1993).

[18] A. Van Wingerde, J. Packer, and J. Wardenier, "New Guidelines for Fatigue Design of HSS Connections," ASCE, Vol. 122 (2) pp. 125-132 (1996).

[19] COSMOS/M, "A Computer Program for Nonlinear Static and Dynamic Analysis," Structural Research and Analysis Corporation, Santa Monica, California, USA (2000).

[20] M. Gibstein, "Parametric Stress Analysis of T. Joints," European Offshore Steels Res. Seminar, Paper No. 26, Cambridge, U.K. (1978).

[21] A. Wordsworth, and G. Smedly, "Stress Concentrations at Unstiffened Tubular Joints," ECSC Seminar, Cambridge, U.K. (1978).

[22] A. Potvin, J. Kuang, R. Leick, and J. Kahlich, "Stress Concentration in Tubular Joints," SPE Journal (1977).

[23] M. Efthymiou, and S. Durkin, "Stress Concentrations in T/Y and Gap/Overlap K-Joints," Proc., BOSS'85: Behavior of Offshore Struct., pp. 429-440 (1985).

Received 21 June, 2004
Accepted 9 September, 2004